Molecular Biology of the Cell
Vol. 16, 3678–3691, August 2005

Functional Role of Syndecan-1 Cytoplasmic V Region in Lamellipodial Spreading, Actin Bundling, and Cell Migration

Ritu Chakravarti,* Vasileia Sapountzi,†‡ and Josephine C. Adams*†

*Department of Cell Biology, Lerner Research Institute, Cleveland Clinic Foundation, Cleveland, OH 44195; and †MRC Laboratory for Molecular Cell Biology and Department of Biochemistry and Molecular Biology, University College London, London WC1E 6BT, United Kingdom

Submitted October 19, 2004; Revised May 11, 2005; Accepted May 25, 2005
Monitoring Editor: Mark Ginsberg

Cell protrusions contribute to cell motility and migration by mediating the outward extension and initial adhesion of cell edges. In many cells, these extensions are supported by actin bundles assembled by the actin cross-linking protein, fascin. Multiple extracellular cues regulate fascin and here we focus on the mechanism by which the transmembrane proteoglycan, syndecan-1, specifically activates lamellipodial cell spreading and fascin-and-actin bundling when clustered either by thrombospondin-1, laminin, or antibody to the syndecan-1 extracellular domain. There is almost no knowledge of the signaling mechanisms of syndecan-1 cytoplasmic domain and we have tested the hypothesis that the unique V region of syndecan-1 cytoplasmic domain has a crucial role in these processes. By four criteria—the activities of N-cadherin/V region chimeras, syndecan-1 deletion mutants, or syndecan-1 point mutants, and specific inhibition by a membrane-permeable TAT-V peptide—we demonstrate that the V region is necessary and sufficient for these cell behaviors and map the molecular basis for its activity to multiple residues located across the V region. These activities correlate with a V-region-dependent incorporation of cell-surface syndecan-1 into a detergent-insoluble form. We also demonstrate functional roles of syndecan-1 V region in laminin-dependent C2C12 cell adhesion and three-dimensional cell migration. These data identify for the first time specific cell behaviors that depend on signaling through the V region of syndecan-1.

INTRODUCTION

Cell adhesion and migration are important for cell and tissue organization in metazoan organisms. Both processes depend critically on the assembly of appropriate cell contact structures that mediate the interaction of cells with their environment. At molecular level, these structures are assembled through the coordinated activation and spatial organization of cell-surface adhesion receptors, intracellular signaling cascades and cytoskeletal components (reviewed by Geiger *et al.*, 2001; Webb *et al.*, 2003). Among the many forms of cell-contacts, cell protrusions are of importance in cell motility and migration by mediating the outward extension of the cell leading edge (reviewed by Adams, 2002; DeMali and Burridge, 2003). This expansion of the plasma membrane is supported by rigid yet elastically flexible actin meshworks that contain parallel F-actin bundles (Svitkina *et al.*, 2003). In many cells, these bundles are cross-linked by the protein fascin. Fascin is under complex regulation in cells, from other actin-binding proteins and from extracellular cues provided by extracellular matrix and polypeptide factors (reviewed by Adams, 2004). The intracellular mechanisms that relay these cues are not widely studied, yet are of general interest for understanding the regulation and function of cell protrusions. In this regard, this laboratory has established that the extracellular glycoprotein, thrombospondin-1 (TSP-1), has distinct activities in inducing cells to form fascin-containing protrusions. This activity of TSP-1 is dependent on the transmembrane proteoglycan, syndecan-1, and can be mimicked by antibody ligation of the syndecan-1 extracellular domain (Adams, 1995; Adams *et al.*, 2001; reviewed by Kureishy *et al.*, 2002).

Syndecan-1 is a member of a gene family of proteoglycans that function in the regulation of cell adhesion, migration, and proliferation in many organisms. For example, overexpression of *Ciona* syndecan mRNA during embryogenesis of *Ciona savignyi* results in delay and impairment of blastopore closure, leading to morphological abnormalities in later embryogenesis such as forking of the tail (Satou *et al.*, 1999). In *Xenopus* embryos, syndecan-2 mediates formation of the left/right axis that is necessary for asymmetric placement of the developing heart (Kramer and Yost, 2002). Gene knockout or overexpression of syndecan-1 result in reduced cell migration during wound-healing and loss of susceptibility to Wnt-mediated mammary tumorigenesis (Alexander *et al.*, 2000; Stepp *et al.*, 2002; Elenius *et al.*, 2004). These complex and yet distinct functions relate to the common and unique attributes of syndecan primary structure. Each family member has a unique extracellular domain sequence, but all

This article was published online ahead of print in *MBC in Press* (http://www.molbiolcell.org/cgi/doi/10.1091/mbc.E04–10–0907) on June 1, 2005.

‡ Present address: Prostate Research Group, Northern Institute for Cancer Research, University of Newcastle Medical School, Newcastle upon Tyne NE2 4HH, United Kingdom.

Address correspondence to: J. C. Adams (adamsj@ccf.org).

Abbreviations used: ECM, extracellular matrix; EGFP, enhanced green fluorescent protein; GAG, glycosaminoglycan; JP, jasplakinolide; MbCD, 6-monodeoxy-6-monoamino-b-cyclodextrin; NCAD, N-cadherin; TSP-1, thrombospondin-1; VBS, vinblastine sulphate.

contain sites for addition of glycosaminoglycan (GAG) chains proximal to the amino-terminus (reviewed by Rapraeger and Ott, 1998; Bernfield *et al.*, 1999). Many functions of syndecans result from their activities as coreceptors through the binding of growth factors to the GAG chains (for example, Kramer and Yost, 2002; Johnson *et al.*, 2004; Steigemann *et al.*, 2004). The transmembrane domains are highly conserved and the short cytoplasmic domains contain two conserved regions, C1 and C2, that have the same sequence in all syndecan family members. C1 and C2 are separated by a variable (V) region that is unique to each syndecan family member but also highly conserved between species orthologues. The C2 region acts as a binding site for PDZ domain-containing proteins and thus links all syndecans to a common set of binding proteins (reviewed by Tkachenko *et al.*, 2005). For syndecan-2 and -4, there is increasing evidence for direct signaling roles of the cytoplasmic domains, that are specifically mediated by the V regions. Serine-phosphorylation within the V region of syndecan-2 is necessary for left/right axis formation in *Xenopus* embryos (Kramer *et al.*, 2002). Syndecan-4 regulates focal adhesion assembly by V-region-dependent activation of protein kinase C (PKC) and binding of α-actinin (reviewed by Couchman, 2003).

In the case of syndecan-1, most attention has focused on its activity as a coreceptor and almost nothing is known about the functions or molecular mechanisms of the cytoplasmic domain apart from the C2 region (reviewed by Rapraeger 2001; Tkachenko *et al.*, 2005). The C1 region is necessary for trafficking of syndecan-1 to the cell-surface (Miettinen *et al.*, 1994). Clustering of the complete transmembrane and cytoplasmic domains in Chinese hamster ovary cells triggers incorporation into a detergent-insoluble membrane fraction and subsequent endocytosis, by an unknown mechanism (Fuki *et al.*, 2000). There are also indications of regulation by tyrosine phosphorylation. Constitutive endogenous tyrosine phosphorylation of syndecan-1 has been reported in certain cells, although the sites of phosphorylation and mechanism of regulation are unknown (Ott and Rapraeger, 1998). Tyrosine 300 has been implicated in the process by which syndecan-1 becomes colocalized with actin microfilaments in long-term adherent cells, but again there is no information on the mechanism (Carey *et al.*, 1996). Thus, the mechanisms of action of syndecan-1 cytoplasmic domain remain almost completely unexplored.

Through our studies of fascin-containing cell protrusions, we have identified dramatic effects of syndecan-1 ligation on lamellipodial spreading and the formation of fascin and actin bundles (Adams *et al.*, 2001). These phenotypes depend on syndecan-1 cytoplasmic domain and provide a robust experimental system with which to examine the mechanism by which the cytoplasmic domain transduces specific cytoskeletal organization. Here, we investigate the hypothesis that the V region has a critical role in this process. We establish that the transduction mechanism depends on the V region independent of the C2 region and define critical amino acids within the V region. We also demonstrate that the V-region-mediated contribution of syndecan-1 to cell protrusions is functionally relevant to ECM adhesion and three-dimensional (3-D) cell migration and depends on its incorporation into a detergent-insoluble fraction. Our findings identify an important novel role of syndecan-1 V region.

MATERIALS AND METHODS

Cells and Other Materials

COS-7 green monkey kidney cells were cultured in DMEM containing 10% fetal calf serum (FCS). C2C12 mouse skeletal myoblasts were grown in DMEM containing 20% FCS. All cells were maintained at 37°C in a humidified 5% CO_2 atmosphere. Mouse syndecan-1 cDNA and the TGM mutant in which the S37, S45, and S47 sites for GAG addition are mutated to alanines were the gifts of Ralph Sanderson (Langford *et al.*, 1998). Chicken N-cadherin (NCAD) cDNA (Hatta *et al.*, 1988) in the pCR3 vector was a gift from Robert Kypta (Imperial College, London). Rat monoclonal antibody (mAb) 281-2 to mouse syndecan-1 core protein (Jalkanen *et al.*, 1985) was obtained from BD Pharmingen (San Diego, CA) in native or biotin-conjugated forms. Antibody ID4 to human syndecan-1 (Bobardt *et al.*, 2004) was from ImmunoKontact (Wiesbaden, Germany). Mouse mAb 55k2 to fascin-1 was obtained from Dako (Glostrup, Denmark). Antibodies to chicken N-cadherin included the mouse mAb FA-5 (Volk *et al.*, 1990; Sigma-Aldrich, Poole, Dorset, United Kingdom), and the rat mAb NCD-2 (Hatta and Takeichi, 1986; Zymed Laboratories, Berlin, Germany). Mouse mAb against β-tubulin, (TUB 2.1-FITC conjugate), was obtained from Sigma-Aldrich. Fluorescein isothiocyanate (FITC)- and tetramethyl rhodamine isothiocyanate- (TRITC) secondary antibodies against mouse immunoglobulins were obtained from ICN Biomedicals (Irvine, CA). Fluorescein-streptavidin was from Vector Laboratories (Burlingame, CA). Phalloidin conjugated to TRITC and secondary antibodies to rat immunoglobulins were obtained from Sigma-Aldrich. Membrane-permeable TAT peptides were synthesized by Genemed Synthesis (South San Francisco, CA) and included TAT only (YGRKKRRQRRR); TAT-V (YGRKKRRQRRRGQANGGAYQKPTKQE); a scrambled control, TAT-Vscr, (YGRKKRRQRRRGQQATGKENAKGYPQ); and a mutant peptide, TAT-VMUT5 (YGRKKRRQRRRGKAANVVAYAKPTGQ). The peptides were synthesized with N-terminal acetylation and C-terminal amidation and were HPLC-purified to >90% purity.

Preparation of Syndecan-1 Mutant and Chimeric Expression Constructs

A series of truncation mutations of mouse syndecan-1 (T1–T4), were prepared by PCR-based mutagenesis of the wild-type cDNA by use of the oligonucleotide primers shown in Table 1 (all oligonucleotides synthesized by Sigma-Genosys). The PCR products of appropriate sizes were cloned into pcDNA3.1/V5-His TOPO mammalian expression vector by the TOPO cloning method according to the manufacturer's procedures (Invitrogen, Carlsbad, CA). Each reverse primer included a stop codon so that the encoded proteins would be expressed in untagged form. S1–T3 and S1–T4 cDNAs were generated by use of S1–T2 as a template. Point mutations were generated in the VC2 region of full-length mouse syndecan-1 in the pcDNA3.1 plasmid by use of QuickChange I or QuickChange II Site-directed mutagenesis kits (Stratagene, La Jolla, CA). The oligonucleotide primers used for each point mutation are shown in Table 1. To create a chimera with N-cadherin (NCAD), the portion of the chicken NCAD coding sequence corresponding to amino acids (aa) 1–759 was amplified by PCR using primers 109F and 105R or 109F and 106R (Table 1). 106R added a *Hpa*I site 3′ to the NCAD cDNA and 105R encoded a stop codon for the negative-control construct, NCADt. The 2280-base pair PCR product was subcloned into pcDNA3.1/V-5-His by TOPO cloning. The chimeric NCADt/syn-1VC2 or NCADt/syn-1V constructs were prepared by insertion of cDNAs encoding either the VC2 portion of mouse syndecan-1 (aa 287–311) or the V region only (aa 287–307) prepared by PCR with primers 107F and 109R, or 107F and 104R, respectively. These primer pairs introduced a *Hpa*I site at the 5′-end and a *Xba*I site at the 3′-end of the cDNAs. After digestion of both VC2 or V and pcDNA3.1/NCADt with *Hpa*I and *Xba*I, VC2 or V cDNA was ligated in frame 3′ to the NCADt cDNA. This procedure inserted a valine (V) and an asparagine (N) residue between NCADt and the syndecan-1 portion. In all cases, the 5′ and 3′ junctions of each new construct and the sites of point mutation were confirmed either by manual DNA sequencing using the dideoxy chain-termination method (Sequenase Version 2.0 DNA sequencing Kit, United States Biological, Swampscott, MA) or by automated DNA sequencing by the CCF Molecular Biotechnology Core (Cleveland, OH) using either standard T7R1 forward and BGH reverse vector primers or an internal primer, 5′AGGAAGGAAGTGCTGGGAGGT. Complete verification that the cDNA sequences did not contain any additional mutations was carried out by automated DNA sequencing, either at MGW Biotech DNA sequencing services (Ebersberg, Germany), or at the CCF Molecular Biotechnology Core, using a set of vector and internal primers to sequence each DNA on both strands. The deletion constructs were first tested for protein expression by in vitro translation, using 1 μg of each DNA template in the Promega TNT T7 Quick coupled Transcription/Translation System (Madison, WI). Translation products were resolved on 12% polyacrylamide gels and syndecan-1 detected by Western blotting with 281-2 mAb, alkaline phosphatase-conjugated anti-rat IgG and enhanced chemiluminescent (ECL) detection as described previously (Adams *et al.*, 2001). In live cells, expression levels of mutant syndecans were compared with the wild-type protein by immunostaining with 281-2 antibody, which is specific to mouse syndecan-1 (Jalkanen *et al.*, 1985), followed by fluorescence-activated cell

Table 1. Oligonucleotides used to prepare syndecan-1 cytoplasmic domain constructs and point mutants

Construct	Primer no.	Oligonucleotide sequence
S1 -T1	LMCB-74F	5′-TCTGGGCAGCATGAGACG-3′
	LMCB-104R	5′-CTACTCCTGCTTGGTGGGTTTCTG-3′
S1-T2	LMCB-74F	5′-TCTGGGCAGCATGAGACG-3′
	LMCB-153R	5′-TTATTTCTGGTAGGCACCGCC-3′
S1-T3	LMCB-74F	5′-TCTGGGCAGCATGAGACG-3′
	LMCB-151R	5′-CTAATTGGCTTGTTTGGGCTC-3′
S1-T4	LMCB-74F	5′-TCTGGGCAGCATGAGACG-3′
	LMCB-152R	5′-TTACTCCTCCAAGGAGTAG-3′
NCADt, with stop codon	LMCB-109F	5′-CTCGCCACCATGTGCCGGATAGCG-3′
	LMCB-150R	5′-CTAACGCTCCTTATCACGGCGCTT-3′
NCADt, with *Hpa*I site	LMCB-109F	5′- CTCGCCACCATGTGCCGGATAGCG-3′
	LMCB-106R	5′-CTAGGTTAACACGCTCCTTATCACGGCGCTT-3′
NCADt/S1VC2	LMCB-107F	5′-GATCGTTAACTCCTTGGAGGAGCCCAAACAA-3′
	LMCB-108R	5′-GATCTCTAGATCAGGCGTAGAACTCCTCCTG-3′
NCADt/S1V with stop codon+ *Hpa*I	LMCB-109F	5′-CTCGCCACCATGTGCCGGATAGCG-3′
	LMCB-104R	5′-CTACTCCTGCTTGGTGGGTTTCTG-3′
S1-K293A	LRI-282F	5′-GAGGAGCCCGCACAAGCCAATGGC-3′
	LRI-283R	5′-GCCATTGGCTTGTGCGGGCTCCTC-3′
S1-Q294A	LRI-284F	5′-GAGGAGCCCAAAGCAGCCAATGGCGG-3′
	LRI-285R	5′-CCGCCATTGGCTGCTTTGGGCTCCTC-3′
S1-N296S/G297V	LMCB-141F	5′-CCCAAACAAGCCAGTTCGGTGCCTACCAG-3′
	LMCB-142R	5′-CTGGTAGGCACCGACACTGGCTTGTTTGGG-3′
S1-G297V/G298V	LMCB-139F	5′-AAACAAGCCAATGTCGTTGCCTACCAGAAA-3′
	LMCB-140R	5′-TTTCTGGTAGGCAACGACATTGGCTTGTTT-3′
S1-A299F	LRI-255F	5′- CAAGCCAATGGCGGTTTCTACAGAAACCCACC-3′
	LRI-256R	5′-GGTGGGTTTCTGGTAGAAACCGCCATTGGCTTG-3′
S1-Y300A	LMCB-93F	5′-AATGGCGGTGCCGCCCAGAAACCCACC-3′
	LMCB-94R	5′-GGTGGGTTTCTGGGCGGCACCGCCATT-3′
S1-Q301A	LRI-257F	5′-GCCAATGGCGGTGCCTACGCGAAACCCACCAAGCAG-3′
	LRI-258R	5′-CTGCTTGGTGGGTTTCGCGTAGGCACCGCCATTGGC-3′
S1-K302G	LRI-271F	5′-GGTGCCTACCAGGGACCCACCAAGCAGGAG-3′
	LRI-272R	5′-CTCCTGCTTGGTGGGTCCCTGGTAGGCACC-3′
S1-K305G	LRI-273F	5′-CAGAAACCCACCGGGCAGGAGGAGTTATAC-3′
	LRI-274R	5′-GTAGAACTCCTCCTGCCCGGTGGGTTTCTG-3′
S1-Q306A	LRI-286F	5′-CAGAAACCCACCAAGGCGGAGGAGTTC-3′
	LRI-287R	5′-GAACTCCTCCGCCTTGGTGGGTTTCTG-3′
S1-E307A	LRI-288F	5′-CCCACCAAGCAGGCGGAGTTCTACGCC-3′
	LRI-289R	5′-GGCGTAGAACTCCGCCTGCTTGGTGGG-3′

sorting (FACS). SDS-PAGE and immunoblotting were carried out as described (Anilkumar *et al.*, 2003).

Transient expression and Syndecan-1 Cytoskeletal Organization Assay

COS-7 or C2C12 cells for transient expression experiments were plated at 25–50% confluency and cotransfected with 3 μg of syndecan-1 expression plasmid DNA and 1 μg of either enhanced green fluorescent protein expression plasmid (EGFPC1, Clontech Laboratories, Heidelberg, Germany) or EGFP-fascin (Adams and Schwartz, 2000) per 60-mm dish by use of Polyfect reagent (Qiagen, Crawley, West Sussex, United Kingdom) according to manufacturer's instructions. Cells were used for experiments 40–42 h after transfection. For the cytoskeletal organization assays, glass coverslips were coated at 4°C overnight with 50 μg/ml 281-2 antibody to mouse syndecan-1, or NCAD antibodies FA-5 or NCD-2, or 50 nM of baculovirus-expressed thrombospondin-1 (TSP-1; Adams *et al.*, 1998), fibronectin (FN; Calbiochem, La Jolla, CA) or EHS laminin (LN; Sigma, St. Louis, MO) and then rinsed in Tris-buffered saline and blocked with 1 mg/ml heat-denatured bovine albumin serum (bovine serum albumin [BSA]) for 1 h. Single-cell suspensions were prepared by release in nonenzymatic cell dissociation medium (Cellgro, Herndon, VA, or Sigma-Aldrich). Cell were washed three times in serum-free DMEM, brought to 3×10^5 cells/ml, and plated on the coated surfaces for 1 h at 37°C in serum-free DMEM. Nonattached cells were removed by rinsing in phosphate-buffered saline (PBS) and the adherent cells were fixed for analysis of cytoskeletal organization as described below. In some assays, cells were pretreated with function-perturbing reagents. Membrane-permeable TAT peptides were added at concentrations from 200 to 2000 nM to the culture media for 1 h before harvesting cells. Pharmacological inhibitors, including the microtubule-perturbing reagents paclitaxel or vinblastine sulfate (VBS; each used at 10–20 μM) or cytochalasin D (10–20 μM) or Y27632 (10–20 nM) were obtained from Calbiochem. These concentrations were established as appropriate for maximal effects on cells and cytoskeleton without toxicity in pilot experiments. Agents were added to the cells for 1 to 2 h before beginning the experiments. All the agents were maintained throughout the experiments at the same concentrations as used for pretreatment.

Immunofluorescence Staining and Morphometric Analysis of Fascin-and-Actin Bundles

For indirect immunofluorescent staining for fascin, cells were fixed in absolute methanol for 10 min. For staining for mouse syndecan-1, cells were fixed in 3.7% formaldehyde. For examination of syndecan-1 extractability, cells were subsequent permeabilized in PBS containing 0.5% Triton X-100. For staining with phalloidin, or tubulin antibodies, cells were fixed in 3.7% formaldehyde for 10 min and then permeabilized for 10 min in O'Neill buffer (50 mM MES, pH 6.1, 5 mM $MgCl_2$, 3 mM EGTA, 100 mM KCl, and 0.2% Triton X-100; O'Neill *et al.*, 1990). Primary antibodies were applied for 90 min, and the cells washed three times in PBS and then stained with appropriate fluorescence-conjugated secondary antibodies. For staining mouse syndecan-1 in adherent cells, cells were incubated with biotinylated 281-2 antibody to syndecan-1 for 90 min, and then with fluorescein-streptavidin for 40 min. All samples were rinsed in PBS and distilled H_2O and mounted on glass microscope slides (BDH, Dagenham, Essex, United Kingdom) in Vectashield mounting medium containing DAPI to visualize DNA and nuclei (Vector Laboratories). Cells labeled with FITC or TRITC fluorochromes were examined by epifluorescence microscope using a Leica DMIRE2 inverted microscope (Heidelberg, Germany) equipped with electronically controlled shutters, filter wheel, and electronic focus. Images were captured under a 63× objective with 1.5× optical magnification with a Hamamatsu camera controller C4742–95 (Bridgewater, NJ), run by Improvision Openlab software (version 3.1.3; Lexington, MA). For quantification of cell area and the length and number of fascin-actin bundles in each cell, digital PICT images were calibrated against a stage micrometer and analyzed morphometrically in Impro-

vision Openlab. Excel worksheets (Microsoft, Redmond, WA) were used to calculate descriptive statistics and to determine significance using unpaired two-tailed *t* tests. The data were prepared for graphical presentation with Prism 4.0 software (Sorrento, CA). Confocal *XY* images were taken under the 63× objective lens (zoom 1 to zoom 3) of a Leica TCS-SP/SP-AOSB laser confocal microscope using Leica confocal software version 2.5. Confocal images of wound-scratch preparations were taken under the 20× objective at zoom 1–3.

Flow Cytometry

Adherent cells (COS-7 or C2C12) were harvested in nonenzymatic cell dissociation solution (Sigma). Cell viability was tested by trypan blue exclusion and the cells were resuspended at 10^7 cells/0.5 ml PBS and incubated with antibody to mouse syndecan-1, chick NCAD, or isotype-matched controls, on ice for 30 min. Cells were washed three times in PBS at 4°C, resuspended in FITC-conjugated secondary antibody, and incubated for 30 min on ice. The cells were washed again in PBS and passed through a Becton Dickinson FACScan (San Jose, CA) using FlowJo software (Tree Star, San Carlos, CA), with fluorescent excitation with an Argon laser (excitation at 488 nm and emission 530 ± 30 nm). The forward and side scatters were gated to exclude small cells, debris, and cell aggregates. Twenty thousand events were acquired per sample. A marker was set 1–2% above the maximum fluorescence of the negative, isotype control-stained cells, and syndecan-1-expressing cells with fluorescence above this level were scored as positively stained. Endogenous syndecan-1 on C2C12 or COS-7 cells was detected by the same procedure. For 3D-migration measurements with transfected C2C12 cells, live C2C12 cells were cotransfected with EGFP and syndecan-1 expression plasmids, or EGFP-fascin, and, after 40 h, sorted for EGFP expression using FACS Vantage and Cellquest software (Becton Dickinson), resuspended in DMEM, and used for experiments. Typically, the population sorted as EGFP-positive was 6% of the total. At least three independent experiments were carried out for each experimental condition.

Wound Healing Migration

C2C12 cells were plated at 2×10^5 cells per p60 tissue culture dishes for 40 h until confluent. The cultures were wounded with a pipette tip, washed, and reincubated with complete medium. Duplicate dishes were harvested at time 0 and at intervals up to 24 h and fixed in 2% paraformaldehyde. Cells were stained for syndecan-1, actin, tubulin, or fascin as described above. The experiment was repeated five times.

Three-dimensional Cell Migration

Polycarbonate filters (NeuroProbe, Cabin John, MD, 8-μm-pore size) were coated with different concentrations (in the range 5 nM–250 nM) of extracellular matrix proteins (laminin, collagen IV, TSP-1, FN) or BSA as a negative control overnight at 4°C and placed in a 96-well chemotaxis chamber (Neuro Probe) containing 85 μl DMEM in the lower chambers. The upper wells were preincubated with 200 μl DMEM. C2C12 cells were preincubated with inhibitory reagents as necessary, harvested, and resuspended at 7.5×10^3 cell/ml in DMEM. One thousand five hundred cells in 200 μl were added to the top chamber and incubated at 37°C in a humidified, 5% CO_2 atmosphere for 4 h. Cells remaining on the top side of the filter were removed with a cotton tip and cells that had migrated to the bottom were fixed with methanol and stained with crystal violet (0.2% in 35% ethanol). Migrated cells were counted under phase-contrast illumination using a 20× objective. Each condition was tested in triplicate in each experiment. Data were pooled from three or more independent experiments and analyzed statistically by unpaired *t* test.

RESULTS

The Role of the Cytoplasmic Domain of Syndecan-1 in Transducing Fascin-and-Actin bundling and Cell Spreading Depends on the V Region

The VC2 regions of syndecan-1 are necessary for transduction of cell spreading and bundling of F-actin by fascin, when the extracellular domain is ligated and clustered either by syndecan-1 antibody or by trimeric TSP-1 (Adams *et al.*, 2001). To determine whether clustering of VC2 alone is sufficient to trigger cytoskeletal organization, we expressed heterologously a chimeric protein consisting of the extracellular, transmembrane, and membrane-proximal region of chicken N-cadherin (N-CAD) fused to the VC2 region of mouse syndecan-1 (designated NCADt/syn1VC2). N-CAD truncated at the same membrane proximal region served as a negative control (designated NCADt; Figure 1A). The two proteins were expressed equivalently in COS-7 cells (Figure 1B) and were expressed similarly on the cell surface (Table 2A). Next, COS-7 cells were cotransfected with the NCAD constructs plus EGFP-fascin and the effect of antibody-mediated clustering of NCAD was quantified according to cell spreading and the assembly of actin-and-fascin bundles. The monoclonal antibodies FA-5 and NCD-2 are specific to chicken N-CAD and bind epitopes close to the N-terminus, within the region responsible for homophilic cadherin binding (Hatta *et al.*, 1986; Volk *et al.*, 1990; reviewed by Gooding *et al.*, 2004). Expression of NCADt supported cell attachment to each of these antibodies but did not result in cell spreading or actin cytoskeletal organization. Cells expressing NCADt/syn1VC2 attached in somewhat greater numbers (mean of 120% relative to the attachment of NCADt-cells, probably because some of the unspread NCADt-expressing cells tend to detach during washing). The individual NCADt/S1VC2-expressing cells spread strongly and assembled fascin-and-actin bundles (Figure 1, C and D, shown for FA-5 antibody only). These phenotypic effects did not depend on expression of EGFP-fascin (unpublished data). These results demonstrate that outside-in clustering of the VC2 region of syndecan-1 at the plasma membrane is suffi-

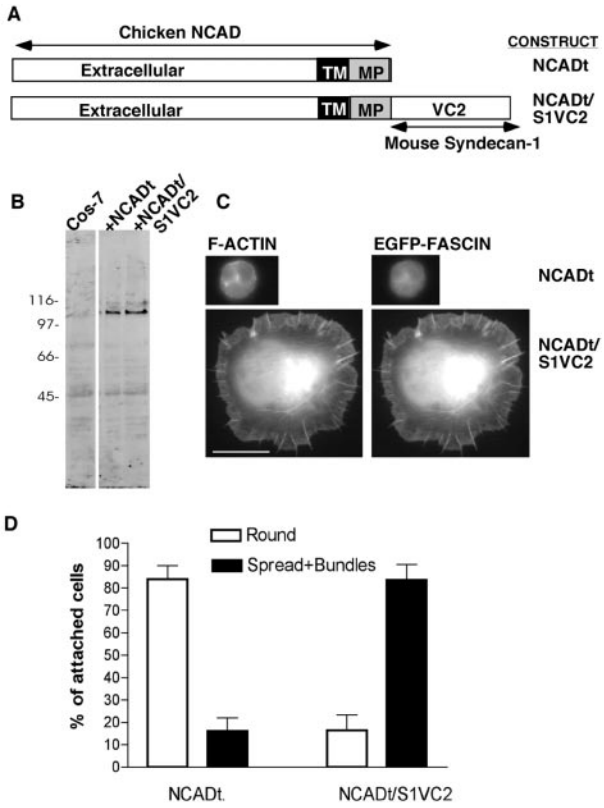

Figure 1. Clustering of the VC2 region of syndecan-1 cytoplasmic domain is sufficient for cell spreading and fascin-and-actin bundling. (A) Schematic diagram of the chimeric constructs prepared. (B) Equivalent expression of the two proteins in COS-7 cells, as determined by immunoblot with antibody specific for chicken NCAD. Molecular mass markers are indicated in kDa. (C) Morphology and F-actin organization of COS-7 cells expressing either NCADt or NCADt/S1VC2 after plating for 1 h on surfaces coated with 50 μg/ml antibody to chick NCAD extracellular domain and staining with phalloidin. Bar, 10 μm. (D) Quantification of the assay from three independent experiments. Each column represents the mean; bars, SEM. Over 1000 cells were scored in total for each construct.

Table 2. Surface expression of syndecan-1 proteins in COS7 or IM-9 myeloma cells determined by live-cell staining and flow cytometry

Sample		% of cells expressing syndecan-1 or heterologous protein	Fluorescent intensity
A	Isotype control	ND	11.6 ± 1.3
	NCADt	86.1 ± 1.9	263.5 ± 19.5
	NCADt.S1VC2	84.5 ± 1.6	211.0 ± 25.0
	NCADt.S1V	84.0 ± 2.0	211.0 ± 26.5
B			
IM9 cells	Isotype control	ND	22.4 ± 0.9
	ID4 (anti-syndecan-1 mab)	94.4 ± 0.7	174.0 ± 7.9
COS-7 cells	ID4 (anti-syndecan-1 mab)	87.0 ± 2.0	46.0 ± 1.0
C	Isotype control	ND	29.7 ± 2.3
	mS1-WT	74.0 ± 6.0	306.6 ± 28.4
	mS1-T1	68.5 ± 13.5	353.9 ± 9.2
	mS1-T2	73.5 ± 9.5	314.0 ± 45.0
	mS1-T3	55.5 ± 5.5	361.5 ± 28.5
	mS1-T4	70.5 ± 9.5	370.4 ± 13.4
D	Isotype control	ND	35.5 ± 2.4
	mSI-WT	47.0 ± 1.4	462.0 ± 74.6
	mS1-K293A	61.5 ± 1.9	620.2 ± 119.0
	mS1-Q294A	56.1 ± 4.1	549.0 ± 119.0
	mS1-N296S/G297V	51.1 ± 9.2	464.8 ±18.8
	mS1-G297V/G298V	49.1 ± 0.3	586.0 ± 32.0
	mS1-A299F	56.9 ± 0.9	509.0 ±117.7
	mS1-Y300A	53.0 ± 5.8	345.0 ± 133
	mS1-Y300E	50.8 ± 1.2	561.0 ± 20.0
	mS1-Q301A	55.0 ± 12.0	440.0 ± 136.0
	mS1-K302A	55.9 ± 3.9	471.0 ± 74.0
	mS1-K305A	56.1 ± 1.6	527.0 ± 88.0
	mS1-Q306A	58.7 ± 4.5	611.8 ± 53.4
	mS1-E307A	53.7 ±13.7	486.7 ± 28.6
	mS1-M4*	47.2 ±2.8	474.0 ± 63.2
	mS1-M5^	59.7 ± 9.2	750.9 ± 65.0
	mS1-M5+Y300E	53.5 ± 3.8	609.0 ± 0.1
	mS1-M5+K302A	56.6 ± 0.5	540.0 ± 106.8
	mS1-M5+Q306A	51.6 ± 1.0	497.0 ± 106.0

Values are mean ± SEM from 3–5 experiments. ND, not determined.

cient to activate fascin-and-actin bundling and cell spreading.

As a first approach to distinguish requirements for the V or C2 regions in these processes, we prepared a set of four C-terminal truncation mutants of mouse syndecan-1 that deleted either the C2 region alone or C2 plus portions of the V region (Figure 2A). COS-7 cells express endogenous syndecan-1 at a low level compared with myeloma cells, which are known for strong expression of syndecan-1 (reviewed by Sanderson and Borset, 2002; Table 2B). All the mouse syndecan-1 deletion proteins were expressed equivalently to wild-type mouse syndecan-1 on the surface of COS-7 cells (Table 2C). We previously demonstrated that expression of wild-type mouse syndecan-1 in COS-7 cells enables cell attachment and lamellipodial spreading on surfaces coated with antibody to the extracellular domain of mouse syndecan-1, in comparison to vector-control cells, which attach only at same level as on BSA-coated surfaces and do not spread (Adams *et al.,* 2001). Cells expressing the truncations T3 and T4 were significantly decreased in cell spreading relative to wild-type syndecan-1. T2-expressing cells maintained a partial capacity to assemble fascin-and-actin bundles, and bundling was significantly decreased in the T3- and T4-expressing cells (Figure 2B). These findings indicated that the C2 motif is not essential for these cytoskeletal responses and implicated the portion of the V region up to the T3 deletion site in mediating the cell behaviors. To confirm that the V region alone is sufficient, we compared the ability of an NCAD chimera containing only the V region of syndecan-1, NCADt/syn1V, to support cell spreading and actin-bundling. Strikingly, NCADt/syn1V supported cell spreading and actin bundling on NCAD antibody surfaces to the same level as NCADt/syn1VC2 (Figure 2B). The cell-attachment activity of the two proteins was equivalent (unpublished data). These results identify a critical requirement for the V region in the mechanism of transduction of spreading and cytoskeletal organization by syndecan-1.

Identification of Critical Determinants for Cell Spreading and Fascin-and-Actin Bundling within the V Region of Syndecan-1

To identify the molecular basis for this activity of the V region, we prepared a series of point mutations in the context of full-length mouse syndecan-1. The choice of mutation sites was informed by our results with the deletion mutants (Figure 2B), multiple sequence alignment of the cytoplasmic domains of vertebrate syndecans (Figure 3A), and consideration of the NMR structure of syndecan-4 cytoplasmic domain peptides (Shin *et al.,* 2001). The multiple sequence alignment documents three key points about the cytoplasmic domains of syndecans, two of which have been widely discussed: 1) the complete conservation of the C1 and C2

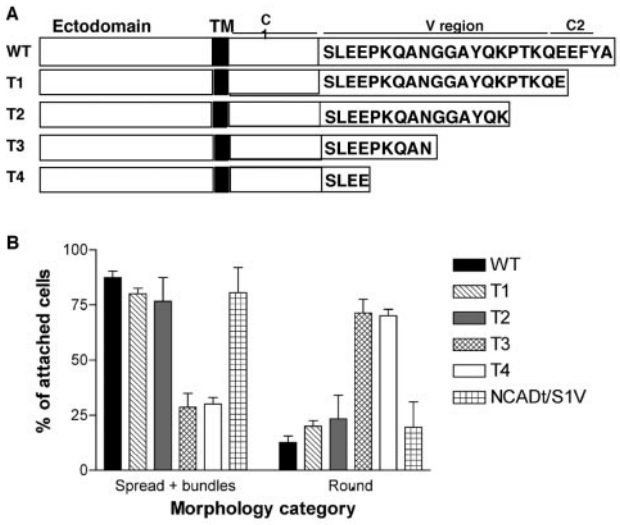

Figure 2. The V region of syndecan-1 cytoplasmic domain is necessary for cell spreading and fascin-and-actin bundling. (A) Schematic diagram of the syndecan-1 deletion constructs prepared. (B) Quantification of transfected COS-7 cell spreading and fascin-and-actin bundling activities in syndecan-1 or NCAD adhesion assays. Each column shows the mean ± SEM for data from five independent experiments. One hundred cells were scored in each experiment.

regions across the whole syndecan family; and 2) the closer sequence similarity between the V regions of syndecan subfamily members (i.e., between syndecan-1 and -3, vs. syndecan-2 and -4; reviewed by Bernfield *et al.,* 1999; Couchman, 2003). An additional third feature that we noted from the alignment was that even within the V regions, certain residues are highly conserved across the family (asterisked in the figure), whereas the central regions of syndecans-1, -2, and -3 contain distinct sequences and can be considered hypervariable. Syndecan-4 has the shortest cytoplasmic domain, and although its V region aligns overall with that of syndecan-2, a distinct central motif is not apparent (Figure 3A).

We prepared single point mutations across the region aa 293–307 of mouse syndecan-1 and included double point mutations within the hypervariable region. We included K293 and Q294 in the screen because K189 and K190 of syndecan-4 (which align with K293 and Q294 of syndecan-1) are involved in ionic interactions that stabilize syndecan-4 cytoplasmic domain as an intertwined dimer (Shin *et al.,* 2001). Syndecan-1 cytoplasmic domain peptides do not dimerize (Oh *et al.,* 1997); however, we wanted to consider the significance of possible ionic interactions of K293 and Q294. Most target residues were substituted with alanine residues, but where the natural residue was a small amino acid (e.g., A299), an amino acid from the same charge group with a large side group was substituted. Y300 has been implicated as a possible site of tyrosine phosphorylation that affects the colocalization of syndecan-1 with F-actin (Carey *et al.,* 1996); therefore both Y300A and Y300E point mutations were prepared. All the V region point mutants were expressed on the cell-surface of COS-7 cells at levels equivalent to or slightly higher than wild-type syndecan-1 (Table 2D).

We quantified the activity of the V region mutants in the syndecan-1 antibody adhesion assay in comparison to wild-type syndecan-1 by scoring three morphometric parameters: cell area, the number of fascin-and-actin bundles per cell, and the length of the fascin-and-actin bundles assembled by each cell (as illustrated in Figure 3B). These analyses uncovered that mutations at multiple sites partially inhibited the F-actin-organizational activities of syndecan-1. For cells expressing wild-type syndecan-1, the mean cell area was 896 ± 79 μm^2, the mean number of actin-and–fascin bundles per cell was 38 ± 2, and the mean length of the bundles was 5.26 ± 0.21 μm (n = 90 cells scored from 6 independent

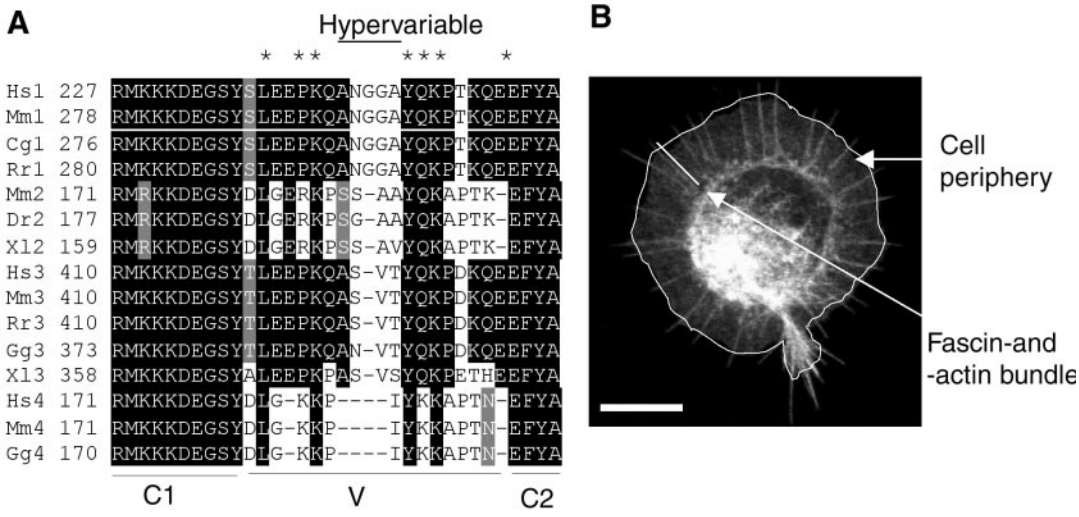

Figure 3. Identification of critical residues within the V region of syndecan-1. (A) ClustalW multiple sequence alignment of the cytoplasmic domains of vertebrate syndecans. Black shading shows identical amino acids; gray indicates conservative substitutions and no shading indicates unrelated amino acids. Cg, *Cricetulus griseus*; Dr, *Danio rerio*; Gg, *Gallus gallus;* Hs, *Homo sapiens*; Mm, *Mus muscularis*; Rn, *Rattus norvegicus*; Xl, *Xenopus laevis*. Asterisk indicate conserved positions within the V region. (B) Morphometric scoring parameters used in the experiments with syndecan-1 point mutants transfectants. COS-7 cells expressing EGFP-fascin and mouse syndecan-1, adherent on antibody to mouse syndecan-1, were scored for cell area (white outline) and the number and length of fascin-containing bundles (white bar) using Openlab software. Bar, 10 μm.

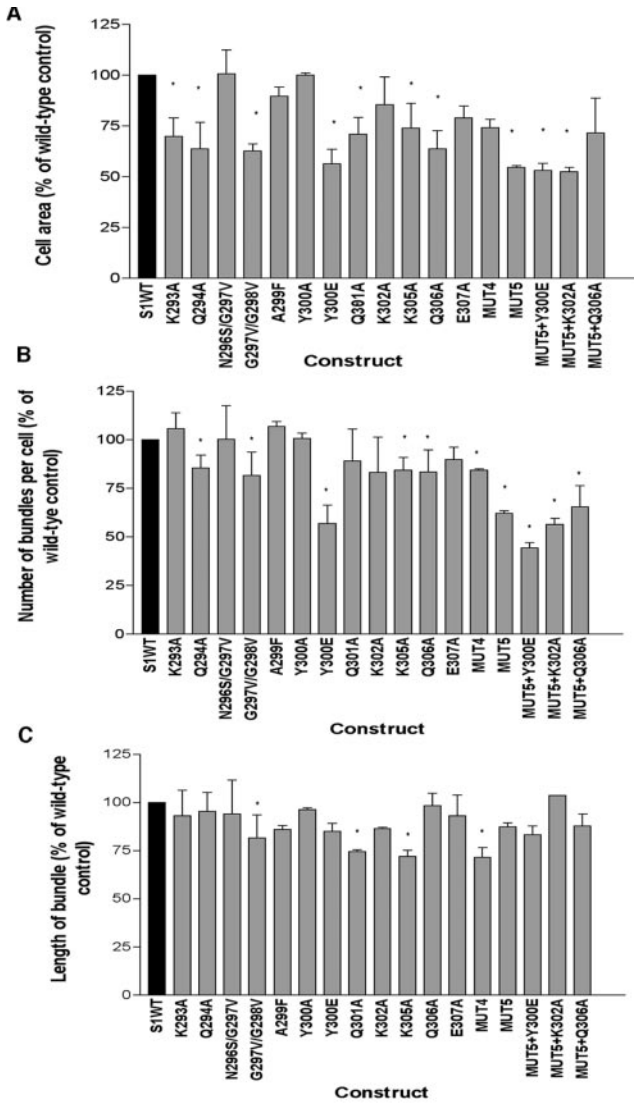

Figure 4. Identification of critical residues within the VC2 region of syndecan-1. Quantification of the effects of syndecan-1 point mutants on COS-7 cell spreading and fascin-and-actin bundling in the syndecan-1 adhesion assay. (A) cell area; (B) number of fascin-and-actin bundles per cell; (C) length of fascin-and-actin bundles. Each column shows the mean ± SEM for data pooled from at least three independent experiments. * Significantly different from wild type at $p \leq 0.002$.

experiments). The most significant effects, corresponding to about a 40% decrease in cell area, were caused by the mutations Q294A, G297V/G298V, Y300E, or Q306A (Figure 4A). The Y300A mutation had activity similar to that of wild-type syndecan-1 (Figure 4A). Certain other mutations: K293A, Q301A, K305A, and E307A, decreased cell area by 25–30%. The number of fascin-and-actin bundles per cell was most strongly decreased by the Y300E mutation (Figure 4B, significantly different from wild-type at $p = 0.0003$), and expression of the mutations Q294A, G297V/G298V, K302A, K305A, and Q306A all resulted in minor decreases in the number of bundles per cell. The residual actin and fascin bundles formed by cells expressing mutant syndecans were similar in length to those formed by cells expressing wild-type syndecan-1 (Figure 4C). Only the G297V/G298V, Q301A, or K305A mutants consistently resulted in the assembly of actin-and-fascin bundles that were modestly but significantly shorter (Figure 4C).

We next investigated the combined effects of the point mutations that resulted in the most impaired activity: that is, Q294, G297V/G298V, Y300E, and K305. Expression of the mutant combination S1:Q294A/G297V/G298V/K305A (designated S1MUT4) resulted in significantly decreased cell area, number of fascin-and-actin bundles, and length of the bundles relative to wild-type syndecan-1; however, the percentage decreases in cell area or number of bundles were no greater than the effects of the functionally compromised single point mutations (Figure 4, A–C). We therefore included an additional mutation in the S1MUT4 construct. S1MUT5 (S1:Q294A/G297V/G298V/Q301A/K305A) was clearly less active with regard to cell spreading and the number of fascin-and-actin bundles per cell (Figure 4, A–C). Out of several additional mutants prepared within the MUT5 construct, S1MUT5+Y300E was the least active: cell area was reduced by 50% (significant at $p = 0.0001$) and the number of fascin and actin bundles per cell by 60% (significant at $p = 0.00003$) relative to cells expressing wild-type syndecan-1 (Figure 4, A–C). The reduced activity of S1MUT5+Y300E was specific to the introduction of the Y300E point mutation because S1MUT5+Q306A or S1MUT5+K302A were not significantly different in activity to MUT5 (Figure 4, A–C). Interestingly, none of the combination mutants differed significantly from single point mutants with regard to the length of the residual fascin-and-actin bundles (Figure 4C). These results identify major roles of syndecan-1 V region in transducing cell spreading and the initiation of fascin-and-actin bundling.

Inhibition of Cell Spreading and Fascin-and-Actin Bundling by a V-region-containing Peptide

The importance of the V region in the mechanism of transducing spreading and actin bundle organization was substantiated by a third independent methodology, that of examining the effects of a membrane-permeable synthetic peptide consisting of the 12-residue polybasic, membrane-penetrating region of the HIV TAT protein and the syndecan-1 V region, TAT-S1V. TAT peptides are widely used as soluble, membrane-permeable competitors of intracellular protein-protein interactions (Becker-Hapak *et al.*, 2001). TAT-S1V peptide entered COS-7 cells with high efficiency within a 1-h period and without any effect on cell viability at concentrations below 2 μM (unpublished data). Cells treated with TAT-S1V showed a concentration-dependent decrease in syndecan-1-activated spreading, with at maximum a 46% reduction in cell area (Figure 5A) and a 25% reduction in the numbers of actin-and-fascin bundles (Figure 5B). The length of the remaining bundles was decreased by 30%, from a mean of 5.0 ± 0.4 to 4 ± 0.7 μm (Figure 5C). Cells treated with TAT peptide containing a scrambled V region sequence, TAT-S1Vscr, or TAT peptide alone, were indistinguishable from untreated control cells for all three parameters (Figure 5, A–C). A TAT-peptide containing the syndecan-1 V sequence mutated at five of the positions that have the greatest combined effect in inhibiting the activities of full-length syndecan-1, TAT-S1VMUT5, was also inactive (Figure 5, A–C).

V region-dependent Transduction of Cytoskeletal Responses Depends on a Detergent-insoluble Form of Cell-surface Syndecan-1

Having identified a novel specific requirement for the V region in the mechanism of cytoskeletal organization by

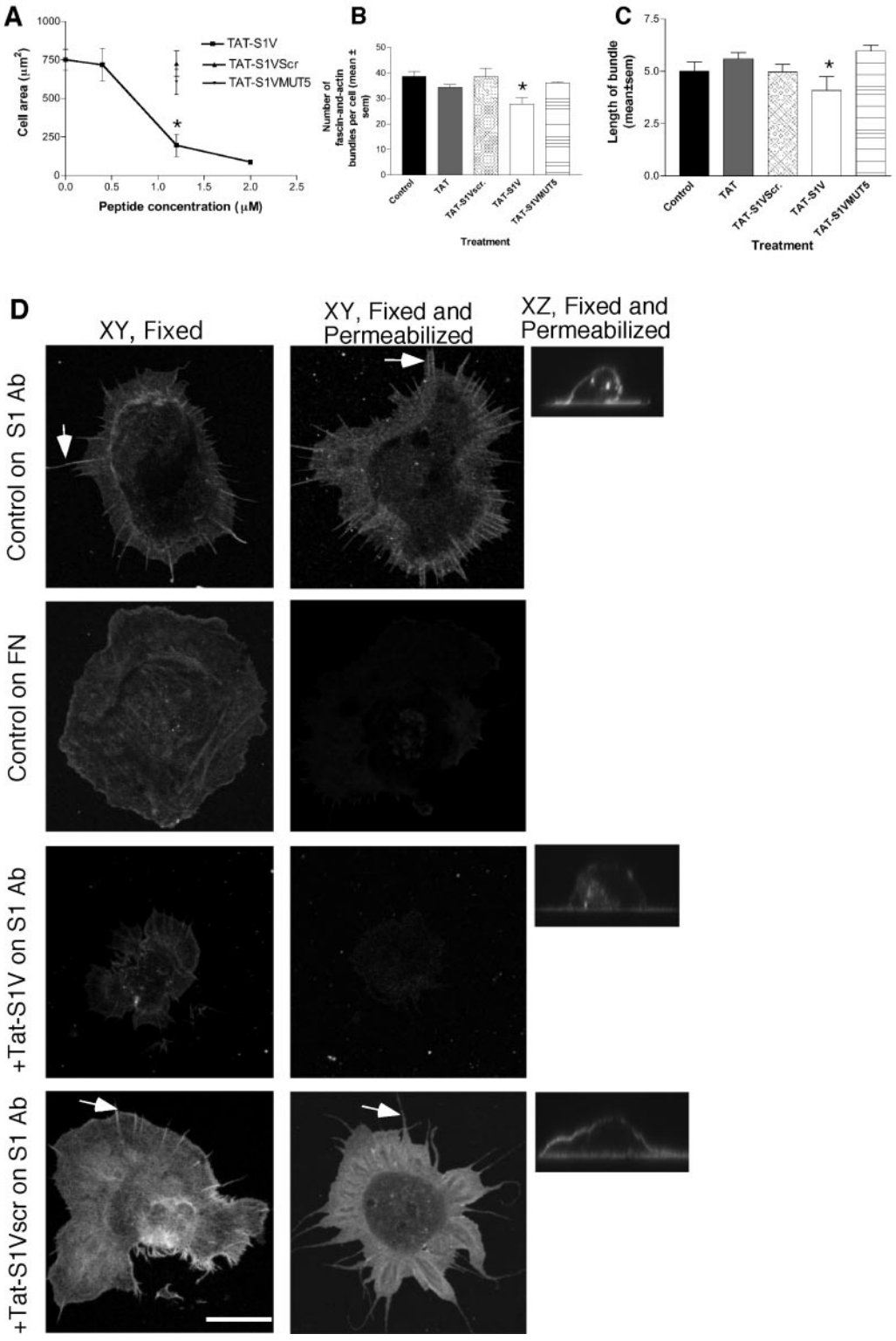

Figure 5. Effect of a membrane-permeable TAT-S1V peptide on cell spreading and syndecan-1 extractability. Transfected COS-7 cells were preincubated with TAT peptides, as indicated, for 1 h before harvesting. Syndecan-1 adhesion assays were carried out for 1 h in the continued presence of peptide. (A–C) Quantification of the effects of TAT peptides on cell spreading and fascin-and-actin bundling. Each graph data point or column indicates the mean ± SEM for data from five independent experiments. In B and C, each peptide was used at 1200 nM. *Significantly different from untreated control at $p \leq 0.001$. (D) Effects of TAT peptides on detergent extractability of syndecan-1. Cells were prepared either fixed or fixed and permeabilized. Mouse syndecan-1 was detected on the adherent cells with biotin-conjugated primary antibody and FITC-conjugated streptavidin, and cells were analyzed by confocal XY and XZ images. Arrow indicates example of alignment of syndecan-1 at sites of F-actin bundles. Each peptide was used at 1200 nM. Under control conditions, ligated syndecan-1 was specifically resistant to extraction (top row), and this property was specifically inhibited by TAT-S1V peptide (third row). Results shown are representative of five independent experiments. Bar, 10 μm.

syndecan-1, we took further steps to analyze its mechanism of action. Because the clustering of syndecan-1 transmembrane and cytoplasmic domains has been reported to result in incorporation into a detergent-insoluble fraction (Fuki *et al.,* 2000), we examined how different states of cytoskeletal organization correlate with detergent-solubility of syndecan-1. In cells expressing wild-type mouse syndecan-1, adherent on syndecan-1 antibody, syndecan-1 had a diffuse localization across the lamellipodia and cell bodies of nonpermeabilized cells, with some enrichment at sites of F-actin bundles (Figure 5D, top row, and unpublished data). Cell-surface syndecan-1 was retained after detergent-extraction of the cells, as demonstrated in *XZ* sections (Figure 5D, top row, side panel). For comparison, we examined syndecan-1 extractability in cells adherent on fibronectin, where focal adhesions dominate, the actin-bundling activity of fascin is down-regulated and overexpression of syndecan-1 does not alter cell morphology or actin organization (Adams *et al.,* 1999, 2001). Under these conditions, syndecan-1 also had a diffuse distribution on the surface of fixed cells but was completely detergent-extractable upon permeabilization (Figure 5D, second row).

To examine how extractability relates to the activity of the V region, the extractability of syndecan-1 was examined in cells pretreated with the TAT syndecan peptides. Pretreatment of cells with TAT-S1V peptide resulted in near-total detergent-extractability of syndecan-1 (Figure 5D, third row). This effect was specific to TAT-S1V peptide, because pretreatment of cells with TAT, TAT-S1Vscr, or TAT-S1VMUT5 peptides did not result in syndecan-1 extraction upon detergent treatment (Figure 5D, bottom row, shown for TAT-S1Vscr only). From these data, we conclude that the TAT-S1V peptide acts as a specific soluble cytoplasmic inhibitor of interactions of syndecan-1 V region that are normally activated by ligation of the extracellular domain of the core protein and which result in resistance of cell-surface syndecan-1 to detergent extraction in correlation with its activity in promoting cell-spreading and actin-bundling by fascin.

ECM Ligands Regulate the Extractability of Endogenous Cell-surface Syndecan-1 by a V Region-dependent Process

To extend our findings to the physiological ligation of syndecan-1 by ECM ligands, we examined the detergent extractability of the endogenous syndecan-1 of mouse C2C12 skeletal myoblasts plated on individual ECM components. As expected from our previous experiments, direct antibody ligation of syndecan-1 on C2C12 cells resulted in a lamellipodial phenotype with multiple cell protrusions (Adams *et al.,* 2001; Figure 6A). In fixed cells, syndecan-1 was distributed across the cell surface, with concentration on cell protrusions and in alignment with actin filaments (Figure 6A and unpublished data). This cell-surface syndecan-1 was highly resistant to detergent extraction (Figure 6A, XY and XZ). C2C12 cells also tended to have more intracellular syndecan-1 than COS-7 cells (compare Figure 6A with 5D). Cells adherent on EHS laminin, another known ligand of syndecan-1 (Suzuki *et al.,* 2003; Yamashita *et al.,* 2004), which also supports fascin protrusions (Adams, 1997), were more smooth-edged. Cell-surface syndecan-1 was again resistant to detergent-extraction (Figure 6A). C2C12 cells on TSP-1 had elongated or protrusive, ruffling morphologies. Syndecan-1 was distributed over the cell surface, with some concentration on ruffling membranes and was also highly resistant to detergent extraction (Figure 6A).

To establish whether the V region of syndecan-1 participates in the resistance of the cell-surface, ECM-ligated syndecan-1 to extraction, we tested syndecan-1 extractability in laminin-adherent C2C12 cells after treatment with the TAT-syndecan peptides. Pretreatment with TAT-S1Vscr did not alter the ability of C2C12 to attach and spread on laminin, nor did it alter the resistance of cell-surface syndecan-1 to extraction (Figure 6B). In contrast, pretreatment with TAT-S1V resulted in cell-rounding, a patchy distribution of cell-surface syndecan-1 and increased extractability of syndecan-1 (Figure 6B, XY and XZ images). These data implicate the V region of syndecan-1 in the mechanism of cytoskeletal responses activated by physiological ECM ligands of syndecan-1.

Functional Role of the V region of Syndecan-1 in Cell Migration

In view of the roles we had identified for syndecan-1 V region in cytoskeletal organization and adhesion to specific ECM ligands, it was of interest to establish whether the reported function of syndecan-1 in cell migration also depends on the V region. First, we examined the distribution of syndecan-1 in migrating cells. In dense cultures of C2C12 cells where there is little directional cell migration, syndecan-1 was nonpolarized and diffuse (Figure 7A, time 0). When directional cell migration was stimulated by wound-scratch across the culture, the front row of cells initially become flattened, with characteristic lamellipodia and fascin- and actin-containing ruffles at their leading edges and elongated microtubules behind the zone of ruffling (Figure 7A, 2- and 4-h time points). Syndecan-1 was highly concentrated at lamellipodial edges where it colocalized with F-actin at the 2- and 4-h time points (Figure 7A, F-actin/syndecan-1 merged images and unpublished data). By 24 h, cells were less flattened and syndecan-1 was distributed over cell bodies as well as at leading edges (Figure 7A). These observations suggested that syndecan-1 might have a specific role in the initiation of polarized cell migration.

To test this idea, we examined the role of syndecan-1 in 3-D transfilter migration. C2C12 cells and other skeletal myoblasts undergo 2-D haptotactic migration on a number of ECM components, including thrombospondin-1 (TSP-1), fibronectin, and laminin (Adams and Schwartz, 2000 and unpublished data). In various cell types, syndecan-1 is a known ligand of these glycoproteins and also of collagens I and IV (Sanderson *et al.,* 1992; San Antonio *et al.,* 1994; Lebakken and Rapraeger, 1996; Suzuki *et al.,* 2003; Yamashita *et al.,* 2004). C2C12 cells underwent 3-D transfilter migration in response to fibronectin, EHS laminin, TSP-1, or collagen IV. Within a 4-h period and with testing of a broad range of concentrations of each ECM component, EHS laminin produced the highest number of migrating cells, and collagen IV and TSP-1 had the lowest activities at each concentration tested (unpublished data). We therefore focused on migration in response to laminin as the most amenable to experimentation.

In a further set of control experiments, we examined the mode of 3-D cell migration of C2C12 cells. Recent reports have distinguished several forms of 3-D cell migration: fibroblasts undergo ECM-adhesive crawling in combination with proteolytic cleavage of ECM fibrils, whereas lymphocytes and certain tumor cells move by a nonproteolytic gliding, amoeboid motion (Sahai and Marshall, 2003; Wolf *et al.,* 2003). Both modes of migration are susceptible to inhibition by disruption of the actin or microtubule cytoskeletons, but can be distinguished by their sensitivity to Rho-kinase inhibitor: amoeboid motility is not inhibited by Rho-kinase inhibitor, whereas fibroblast-like crawling is (Wolf *et al.,* 2003; Sahai and Marshall, 2003). C2C12 cell

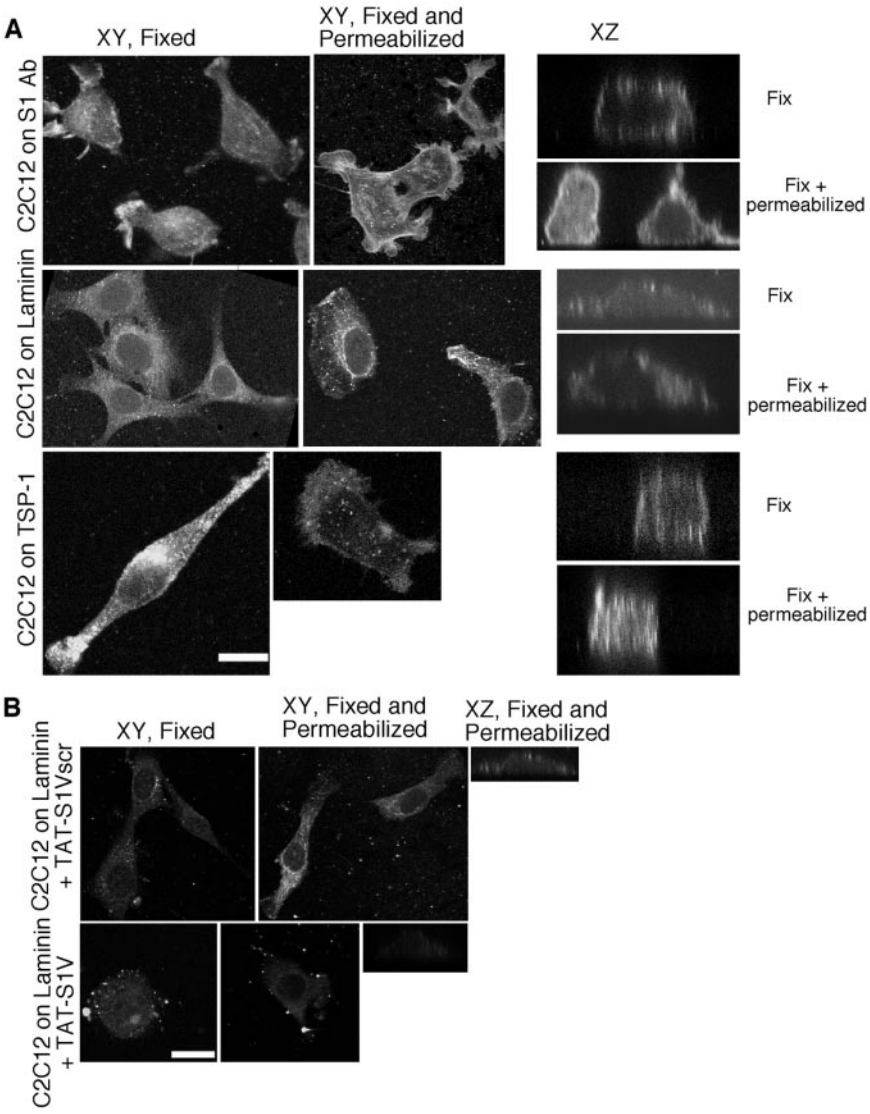

Figure 6. Adhesion to ECM ligands renders endogenous syndecan-1 nonextractable. (A) C2C12 cells were plated on surfaces coated with 50 μg/ml antibody to mouse syndecan-1; 50 nM EHS laminin, or 50 nM TSP-1 for 3 h. Syndecan-1 extractability was assessed by staining cells with biotin-conjugated primary antibody and FITC-conjugated streptavidin after fixation or after fixation and permeabilization. Cells were viewed as confocal XY or XZ sections. Bar, 10 μm. (B) Treatment with TAT-S1V peptide renders endogenous syndecan-1 detergent-extractable in laminin-adherent C2C12 cells. Cells were pretreated with 1200 nM TAT-S1V or control TAT-S1Vscr peptides for 2 h before adhesion on 50 nM laminin in the continued presence of peptides as described above. Bar, 10 μm.

migration on laminin was completely blocked when cells were treated with cytochalasin D. Perturbation of microtubules, either by paclitaxel or vinblastine, also substantially prevented migration. The Rho-kinase inhibitor Y27632 inhibited migration to the same extent as the actin and microtubule inhibitors (Figure 7B). These results identified that C2C12 cells undergo a fibroblast-like form of 3-D cell migration.

To establish whether syndecan-1 was involved in laminin-induced C2C12 migration, we compared the migration of cells pretreated with either TAT-S1V or control TAT peptides. Although cells treated with TAT-S1Vscr or TAT-S1VMUT5 migrated to the same extent as control cells, the number of cells migrating after TAT-S1V peptide treatment was inhibited by 50% (Figure 7C). Pretreatment of the cells with antibody to syndecan-1 extracellular domain enhanced cell migration in a concentration-dependent manner (Figure 7C). These findings indicated that the activity state of syndecan-1 regulates 3-D laminin-dependent cell migration and that the V region has a role in this process.

To substantiate the mechanistic role of the V region, C2C12 cells were cotransfected with wild-type syndecan-1 or the point mutant forms that we had identified to be most impaired in cytoskeletal-organization activities: Y300E, MUT5, and MUT5+Y300E, and with EGFP to mark the transfected cells. All the syndecan-1 proteins were expressed equivalently on the surface of C2C12 cells (unpublished data). EGFP-positive cells were selected by gated flow cytometric sorting and tested for transfilter migration on laminin. The cells expressing EGFP only or EGFP-fascin had the same migration characteristics as control, untransfected C2C12 cells; however, cells overexpressing wild-type syndecan-1 were markedly reduced in their ability to migrate (Figure 7D, difference to controls significant at $p = 0.005$). The extent of inhibition was as substantial as that obtained by pharmacological disruption of the cytoskeleton (compare Figure 7, B and D). This activity was not due to binding of the GAG chains to laminin, because syndecan-1 mutated at the three heparin sulfate addition sites (TDM mutant; Langford *et al.*, 1998) that retains matrix-attachment activity (Adams *et al.*, 2001) had equivalent activity to wild-type syndecan-1 (Figure 7D).

In contrast, MUT5+Y300E-expressing cells were significantly more migratory than the cells expressing wild-type syndecan-1, indicating that the wild-type V region contributes to the slowing of cell migration by syndecan-1 (Figure

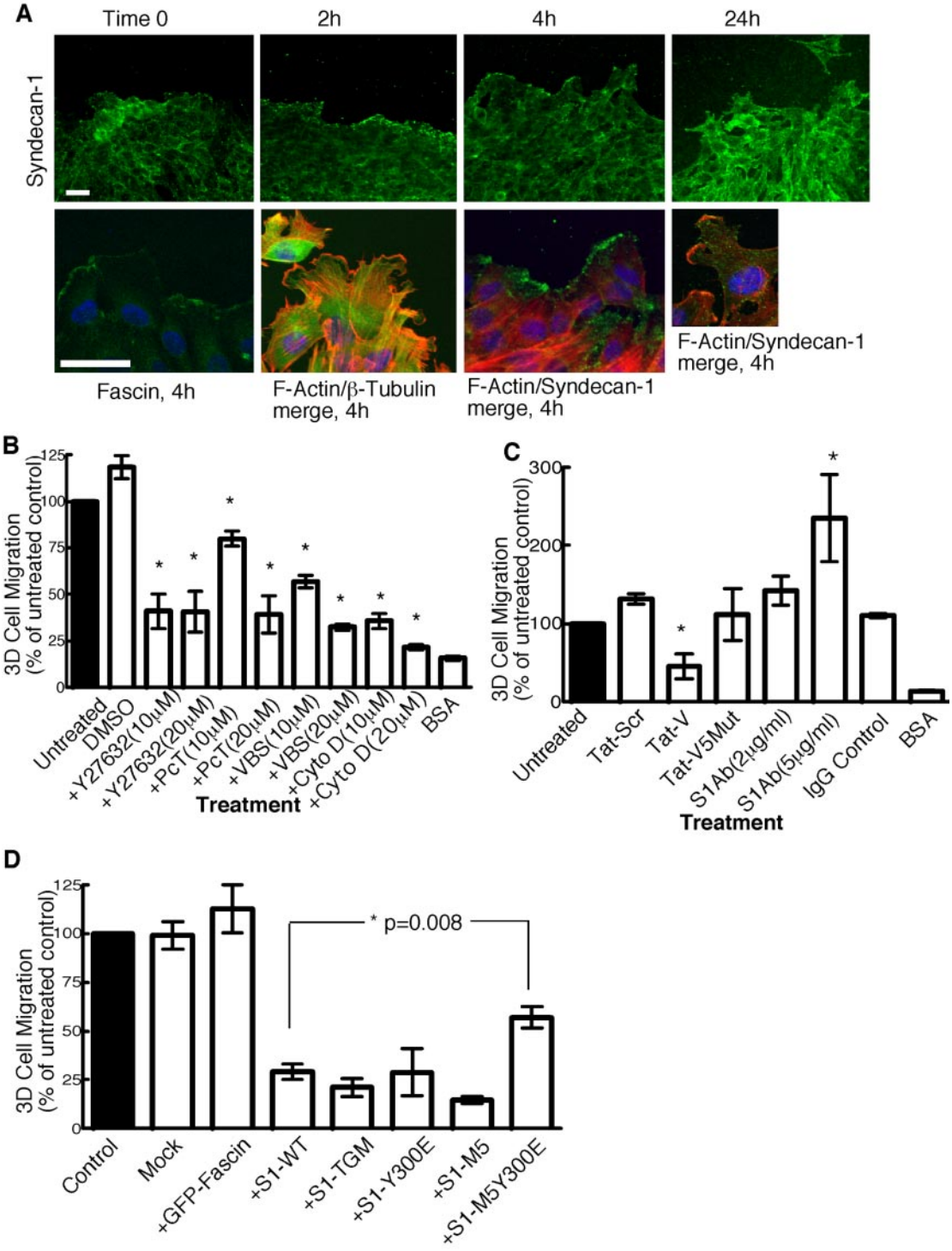

Figure 7. Syndecan-1 localizes to leading edge of migrating cells and has a functional role in 3-D cell migration. (A) C2C12 cells were grown to confluency and wounded with a micropipette tip. At different times after wounding, dishes were fixed, permeabilized, and stained for syndecan-1. At 4 h, syndecan-1 was most concentrated at the front of migrating cells, along with fascin and F-actin. β-tubulin was present behind the ruffling edges. Representative merged images are shown for actin and β-tubulin, and actin and syndecan-1. Bars, 10 μm. (B–D) Quantification of transfilter cell migration assays. Pore filters, 8-μm, were coated with 50 nM EHS laminin or 1 mg/ml BSA. TAT-S1V and TAT-S1Vscr peptides were added at 1200 nM. With the exception of syndecan-1 antibody, which was added only during the assay, C2C12 cells were preincubated with reagents at the concentrations indicated for 1 h and then harvested, and the experiments were carried out in the continued presence of each reagent. Each condition was carried out in triplicate in each experiment, and transfilter migration was scored after 4 h. DMSO, dimethyl sulfoxide; PcT, paclitaxel; VBS, vinblastine sulfate; CytoD, cytochalasin D. In D, C2C12 cells coexpressing wild-type or mutant syndecan-1 and EGFP or EGFP-fascin were sorted by flow cytometry, and 1500 EGFP-positive cells were added to each well coated with 50 nM EHS laminin. After 4 h at 37°C, cells that had migrated to the far side of the filter were fixed, stained, and counted under phase-contrast illumination. Each condition was carried out in triplicate in each experiment. Columns represent mean ± SEM for data from at least three independent experiments.

7D, $p = 0.008$). The Y300E mutation alone reduced cell migration to the same level as wild-type syndecan-1 (Figure 7D). Under each condition, residual cell migration was almost completely inhibited by Y27632, indicating that the mode of cell migration was not altered by the overexpression of syndecan-1 or syndecan-1 V region mutants (unpublished data). These data demonstrate a role for the V region in the modulation of cell migration by syndecan-1.

DISCUSSION

Within the family of mammalian syndecans, syndecan-1 has been linked to the modulation of cell proliferation, migration, and the regulation of the actin cytoskeleton. Thus, syndecan-1 has completely distinct activities from syndecan-4, which cooperates in the assembly of contractile focal adhesions (reviewed by Couchman, 2003), or syndecan-2, which is involved in the assembly of dendritic spines or the ECM (Ethell *et al*., 2001; reviewed by Tkachenko *et al.*, 2005). Although mechanisms of signaling by syndecan-2 and -4 are known to depend on their V regions, there is no knowledge of the specific roles of syndecan-1 V region. In this study, we establish for the first time that critical determinants for transducing cytoskeletal organization in response to antibody ligation or physiological ECM ligands lie within aa 294–307 of the unique V region of syndecan-1. By four criteria (deletion mutants, point mutants, NCAD chimeras, and use of TAT-V peptide), the C2 region is not essential for this activity. We demonstrate that upon ligation and clustering either by antibody or ECM ligands, cell-surface wild-type syndecan-1 enters a detergent-resistant state and that this state depends on the V region. We have also identified a role of the V region in 3-D cell migration.

Our analysis of syndecan-1 deletion mutants focused attention on aa 297–307 as critical for cell spreading and actin bundling (Figure 2). The analysis of point mutations within the V region then revealed a complex functionality of the region. Of the 12 single or double point mutations prepared, 7 resulted in partial impairment of cell spreading and 5 of these also significantly decreased the number of fascin-and-actin bundles (Figure 4). More severe phenotypes were obtained when the most inhibitory mutations were combined together, resulting in similar levels of inhibition of cell spreading and fascin-and-actin bundle assembly. The function-perturbing mutations corresponded to a subset of the amino acids that are conserved across all syndecan V regions and to the unique GG motif within the syndecan-1 V region hypervariable domain (Figure 4A). Further experiments will be needed to establish if these residues are important for the structure of syndecan-1 cytoplasmic domain or for functional protein-protein interactions or both. K189 and K194 of syndecan-4, which align with K293 and K302 of syndecan-1, are important for the ionic interactions by which syndecan-4 cytoplasmic domains form obligate dimers (Shin *et al.*, 2001). Syndecan-1 and -2 cytoplasmic domains do not dimerize in solution (Oh *et al.*, 1997); however, it is likely that all syndecan cytoplasmic domains oligomerize in vivo by lateral interactions as a result of activation and self-association of their extracellular and transmembrane domains (reviewed by Couchman, 2003). Ionic interactions of the conserved positively charged residues could also be important in this process.

The mutation of Y300 to glutamic acid impaired actin organization activity. Constitutive tyrosine phosphorylation of syndecan-1 occurs in lymphoma cell lines, but the residues phosphorylated and functional significance are unknown (Ott and Rapraeger, 1998). Although the Y300E mutation clearly impaired function in our experimental system, the Y300A did not (Figure 4). It is also the case that the surrounding amino acids do not conform to a consensus tyrosine kinase phosphorylation motif (established by search of PROSITE). Thus, the effect of the Y300E mutation is more likely due to the change of charge and side group than to phosphomimetic activity.

Interestingly, the activity of syndecan-1 in lamellipodial spreading and actin bundling correlated with incorporation of syndecan-1 into a detergent-insoluble fraction. This process was specific, because upon cell adhesion to fibronectin that involves a different state of cytoskeletal organization, overexpression of syndecan-1 does not result in alterations to cytoskeletal organization and syndecan-1 is detergent-extractable (Figure 5). Detergent-insolubility of membrane proteins has been related to their incorporation into cholesterol-rich membrane microdomains and to signaling across the plasma membrane (Simon and Ikonen, 1997). Indeed, we have found that cholesterol-depletion by β-methyl cyclodextrin renders cell-surface syndecan-1 constitutively detergent-extractable and results in build-up of intracellular syndecan-1 (unpublished observations). Thus, signaling by syndecan-1 to the cytoskeleton appears to depend on its incorporation into lipid rafts.

An important outcome of our studies was the distinction revealed between effects of syndecan-1 on cell-spreading, the number of fascin-and-actin bundles per cell and the length of any residual bundles. The independent approaches taken to perturb wild-type syndecan-1 function: point mutation of syndecan-1 or use of TAT-S1V peptide consistently had significant effects on cell spreading and the numbers of fascin-and-actin bundles, yet the length of any remaining bundles was consistently less significantly altered (Figures 4 and 5). Both cell spreading and the assembly of fascin-and-actin bundles depend initially on actin nucleation and polymerization. In the spread lamellipodium, actin filaments are assembled as a branched network, in general by the action of Arp2/3 complex (Pollard and Borisy, 2003). Correlated immunofluorescence and electron microscopic analysis has uncovered that fascin and F-actin bundles in the lamellipodia of melanoma cells are initiated from preexisting actin microfilaments within the lamellipodium that become clustered at cell margins by an activity of vasodilator-stimulated phosphoprotein, (VASP), and then elongated into parallel bundles by the cross-linking activity of fascin (Svitkina *et al.*, 2003). The quantitatively distinct effects of syndecan-1 perturbation on cell area and bundle number versus the length of residual bundles in our study strongly imply that syndecan-1 specifically regulates F-actin organization at the level of cell spreading and bundle initiation, with bundle elongation under separate downstream regulation. Thus, any bundles that do initiate under the inhibitory conditions continue to elongate to the same length as in control cells. With regard to the initiation process, we envision that activation of syndecan-1 may recruit and/or activate components necessary for actin nucleation or filament assembly and that the recruitment of fascin to prebundle sites can be controlled separately from its F-actin cross-linking activity. Indeed, we previously placed activation of the known regulators of actin nucleation, Cdc42 and Rac, upstream of TSP-1-induced cell spreading and fascin-and-actin bundle assembly (Adams and Schwartz, 2000). Understanding how actin is assembled and bundles initiate as a result of syndecan-1 signaling will require identification of binding partners of the syndecan-1 V region.

Our data also demonstrate that the activity of syndecan-1 V region is necessary in the physiological responses of cells

to ECM ligands and the regulation of cell migration. In vivo, down-regulation of syndecan-1 on invasive carcinoma cells and up-regulation on tumor-associated fibroblasts are both associated with activation of tumor cell migration (Timar *et al.*, 2002). Either gene knockout or overexpression of syndecan-1 result in reduced cell migration during wound-healing (Stepp *et al.*, 2001; Elenius *et al.*, 2004). Thus, as established for many proteins that function in cell migration (reviewed by Webb *et al.*, 2003), a certain balance of syndecan-1 expression appears to be necessary to support optimal cell migration. We found that the endogenous syndecan-1 of C2C12 cells becomes localized in leading edge ruffles after wounding of a cell monolayer, suggestive of a role in directional cell migration. In agreement with other reports, overexpression of syndecan-1 inhibited 3-D cell migration, probably due to stabilization of cell protrusions leading to decreased adhesion dynamics. We established the role of the V region in this activity by two criteria: specific inhibition of migration involving endogenous syndecan-1 by TAT-V peptide and the much reduced activity of the S1MUT5Y300E protein. We note that the mutant did not completely restore migration to control levels, which suggests that other domains of syndecan-1, for example, the transmembrane and extracellular domain, might contribute to its inhibitory activity (Langford *et al.*, 2005). In summary, we have identified a mechanism for syndecan-1 signaling to specific states of cytoskeletal organization that is dependent on the molecular nature of the V region and on incorporation of syndecan-1 into a detergent-insoluble form.

ACKNOWLEDGMENTS

We thank Alexia Zaromytidou for initial experiments with truncated syndecan-1, Robert Kypta for the gift of chicken NCAD cDNA, Cathy Shemo and the CCF Flow Cytometry core, Dmitry Leontiev and Amit Vasanji for confocal microscopy training and assistance, and the CCF Molecular Biotechnology core for DNA sequencing. Research in London was supported by the Wellcome Trust (SFBBR 038284 to J.C.A.). Research in USA was supported by National Institutes of Health Grant GM068073.

REFERENCES

Adams, J. C. (1995). Formation of stable microspikes containing actin and the 55kDa actin-bundling protein, fascin, is a cosequence of cell adhesion to thrombospondin-1: implications for the anti-adhesive activities of thrombospondin-1. J. Cell Sci. *108*, 1977–1990.

Adams, J. C. (1997). Characterization of cell-matrix adhesion requirements for the formation of fascin microspikes. Mol. Biol. Cell *8*, 2345–2363.

Adams, J. C. (2002). Regulation of protrusive and contractile cell-matrix contacts. J. Cell Sci. *115*, 257–265.

Adams, J. C. (2004). Roles of fascin in cell adhesion and motility. Curr. Opin. Cell Biol. *16*, 590–596.

Adams, J. C., Clelland, J. D., Collett, G. D., Matsumura, F., Yamashiro, S., and Zhang, L. (1999). Cell-matrix adhesions differentially regulate fascin phosphorylation. Mol. Biol. Cell *10*, 4177–4190.

Adams, J. C., Kureishy, N., and Taylor, A. L. (2001). A role for syndecan-1 in coupling fascin spike formation by thrombospondin-1. J. Cell Biol. *152*, 1169–1182.

Adams, J. C., and Schwartz, M. A. (2000). Stimulation of fascin spikes by thrombospondin-1 is mediated by the GTPases Rac and Cdc42. J. Cell Biol. *150*, 807–822.

Adams, J. C., Seed, B., and Lawler, J. (1998). Muskelin, a novel intracellular mediator of cell adhesive and cytoskeletal responses to thrombospondin-1 Embo J. *17*, 4964–4974.

Alexander, C. M., Reichsman, F., Hinkes, M. T., Lincecum, J., Becker, K. A., Cumberledge, S., and Bernfield, M. (2000). Syndecan-1 is required for Wnt-1-induced mammary tumorigenesis in mice. Nat. Genet. *25*, 329–332.

Anilkumar, N., Parsons, M., Monk, R., Ng, T., and Adams, J. C. (2003). Interaction of fascin and protein kinase Calpha: a novel intersection in cell adhesion and motility. EMBO J. *22*, 5390–5402.

Becker-Hapak, M., McAllister, S. S., and Dowdy, S. F. (2001). TAT-mediated protein transduction into mammalian cells. Methods *24*, 247–256.

Bernfield, M., Gotte, M., Park, P. W., Reizes, O., Fitzgerald, M. L., Lincecum, J., and Zako, M. (1999). Functions of cell surface heparan sulfate proteoglycans. Annu. Rev. Biochem. *68*, 729–777.

Bobardt, M. D., Salmon, P., Wang, L., Esko, J. D., Gabuzda, D., Fiala, M., Trono, D., Schueren, B. V., David, G., and Gallay, P. A. (2004). Contribution of proteoglycans to human immunodeficiency virus type 1 brain invasion. J. Virol. *78*, 6567–6584.

Carey, D. J., Bendt, K. M., and Stahl, R. C. (1996). The cytoplasmic domain of syndecan-1 is required for cytoskeleton association but not detergent insolubility. J. Biol. Chem. *271*, 15253–15260.

Couchman, J. R. (2003). Syndecans: proteoglycan regulators of cell-surface microdomains? Nat. Rev. Mol. Cell. Biol. *4*, 926–937.

DeMali, K. A., and Burridge, K. (2003). Coupling membrane protrusion and cell adhesion. J. Cell Sci. *116*, 2389–2397.

Elenius, V., Gotte, M., Reizes, O., Elenius, K., and Bernfield, M. (2004). Inhibition by the soluble syndecan-1 ectodomains delays wound repair in syndecan-1 overexpressing mice. J. Biol. Chem. *279*, 41928–41935.

Ethell, I. M., Irie, F., Kalo, M. S., Couchman, J. R., Pasquale, E. B., and Yamaguchi, Y. (2001). EphB/syndecan-2 signaling in dendritic spine morphogenesis. Neuron. *31*, 1001–1113.

Fuki, L., Meyer, M. E., and Williams, K. J. (2000). Transmembrane and cytoplasmic domain of syndecan mediate a multi-step endocytic pathway involving detergent-insoluble membrane rafts. Biochem. J. *351*, 607–612.

Geiger, B., Bershadsky, A., Pankov, R., and Yamada, K. M. (2001). Transmembrane crosstalk between the extracellular matrix–cytoskeleton crosstalk. Nat Rev. Mol. Cell. Biol. *11*, 793–805.

Gooding, J. M., Yap, K. L., and Ikura, M. (2004). The cadherin–catenin complex as a focal point of cell adhesion and signalling: new insights from three-dimensional structures. Bioessays *26*, 497–511.

Hatta, K., Nose, A., Nagafuchi, A., and Takeichi, M. (1988). Cloning and expression of cDNA encoding a neural calcium-dependent cell adhesion molecule: its identity in the cadherin gene family. J. Cell Biol. *106*, 873–881.

Hatta, K., and Takeichi, M. (1986). Expression of N-cadherin adhesion molecules associated with early morphogenetic events in chick development. Nature *320*, 447–449.

Jalkanen, M., Nguyen, H., Rapraeger, A., Kurn, N., and Bernfield, M. (1985). Heparan sulphate proteoglycans from mouse mammary epithelial cells: localisation on the cell surface with a mAb. J. Cell Biol. *101*, 976–984.

Johnson, K. G., Ghose, A., Epstein, E., Lincecum, J., O'Connor, M. B., and Van Vactor, D. (2004). Axonal heparan sulfate proteoglycans regulate the distribution and efficiency of the repellent slit during midline axon guidance. Curr. Biol. *14*, 499–504.

Kramer, K. L., Barnette, J. E., and Yost, H. J. (2002). PKCgamma regulates syndecan-2 inside-out signaling during *Xenopus* left-right development. Cell *111*, 981–990.

Kramer, K. L., and Yost, H. J. (2002). Ectodermal syndecan-2 mediates left-right axis formation in migrating mesoderm as a cell-nonautonomous Vg1 cofactor. Dev. Cell *2*, 115–124.

Kureishy, N., Sapountzi, V., Prag, S., Anilkumar, N., and Adams, J. C. (2002). Fascins, and their roles in cell structure and function. Bioessays *24*, 350–361.

Langford, J. K., Stanley, M. J., Cao, D., and Sanderson, R. D. (1998). Multiple heparan sulfate chains are required for optimal syndecan-1 function. J. Biol. Chem. *273*, 29965–29971.

Langford, J. K., Yang, Y., Kieber-Emmons, T., and Sanderson, R. D. (2005). Identification of an invasion regulatory domain within the core protein of syndecan-1. J. Biol. Chem. *280*, 3467–3473.

Lebakken, C. S., and Rapraeger, A. C. (1996). Syndecan-1 mediates cell spreading in transfected human lymphoblastoid (Raji) cells. J. Cell Biol. *132*, 1209–1221.

Miettinen, H. M., Edwards, S. N., and Jalkanen, M. (1994). Analysis of transport and targeting of syndecan-1, effect of cytoplasmic tail deletions. Mol. Biol. Cell *5*, 1325–1339.

Oh, E. S., Woods, A., and Couchman, J. R. (1997). Multimerisation of the cytoplasmic domain of syndecan-4 is required for its ability to activate PKC. J. Biol. Chem. *272*, 11805–11811.

O'Neill, C., Jordon, P., Riddle, P., and Ireland, G. (1990). Narrow linear strips of adhesive substratum are powerful inducers of both growth and total focal contact area. J. Cell Sci. *95*, 577–586.

Ott, V. L., and Rapraeger, A. C. (1998). Tyrosine phosphorylation of syndecan-1 and -4 cytoplasmic domains in adherent B82 fibroblasts. J. Biol. Chem. *273*, 35291–35298.

Pollard, T. D., and Borisy, G. G. (2003). Cellular motility driven by assembly and disassembly of actin filaments. Cell *112*, 453–465.

Rapraeger, A. C. (2001). Molecular interactions of syndecans during development. Semin. Cell Dev. Biol. *12*, 107–116.

Rapraeger, A. C., and Ott, V. L. (1998). Molecular interactions of the syndecan core proteins. Curr. Opin. Cell Biol. *10*, 620–628.

Sahai, E., and Marshall, C. J. (2003). Differing modes of tumour cell invasion have distinct requirements for Rho/ROCK signalling and extracellular proteolysis. Nat. Cell Biol. *5*, 711–719.

San Antonio, J. D., Karnovsky, M. J., Gay, S., Sanderson, R. D., and Lander, A. D. (1994). Interactions of syndecan-1 and heparin with human collagens. Glycobiology *4*, 327–332.

Sanderson, R. D., and Borset, M. (2002). Syndecan-1 in B lymphoid malignancies. Ann. Hematol. *81*, 125–135.

Sanderson, R. D., Sneed, T. B., Young, L. A., Sullivan, G. L., and Lander, A. D. (1992). Adhesion of B lymphoid (MPC-11) cells to type I collagen is mediated by integral membrane proteoglycan, syndecan. J. Immunol. *148*, 3902–3911.

Satou, Y., Chiba, S., and Satoh, N. (1999). Expression cloning of an ascidian syndecan suggests its role in embryonic cell adhesion and morphogenesis. Dev. Biol. *211*, 198–207.

Shin, J., Lee, W., Lee, D., Koo, B.-K., Han, I., Lim, Y., Woods, A., Couchman, J. R., and Oh, E.-S. (2001). Solution structure of the dimeric cytoplasmic domain of syndecan-4. Biochemistry *40*, 8471–8478.

Simon, K., and Ikonen, E. (1997). Functional rafts in cell membranes. Nature *387*, 569–572.

Steigemann, P., Molitor, A., Fellert, S., Jackle, H., and Vorbruggen, G. (2004). Heparan sulfate proteoglycan syndecan promotes axonal and myotube guidance by slit/robo signaling. Curr. Biol. *14*, 225–230.

Stepp, M. A. *et al.* (2002). Defects in keratinocyte activation during wound healing in the syndecan-1-deficient mouse. J. Cell Sci. *115*, 4517–4531.

Suzuki, N. *et al.* (2003). Syndecan binding sites in the laminin alpha1 chain G domain. Biochemistry *42*, 12625–12633.

Svitkina, T. M., Bulanova, E. A., Chaga, O. Y., Vignjevic, D. M., Kojima, S., Vasiliev, J. M., and Borisy, G. G. (2003). Mechanism of filopodia initiation by reorganization of a dendritic network. J. Cell Biol. *160*, 409–421.

Timar, J., Lapis, K., Dudas, J., Sebestyen, A., Kopper, L., Kovalszky, I. (2002). Proteoglycans and tumor progression: Janus-faced molecules with contradictory functions in cancer. Semin. Cancer Biol. *12*, 173–186.

Tkachenko, E., Rhodes, J. M., and Simons, M. (2005). Syndecans: new kids on the signaling block. Circ. Res. *96*, 488–500.

Volk, T., Volberg, T., Sabanay, I., and Geiger, B. (1990). Cleavage of A-CAM by endogenous proteinases in cultured lens cells and in developing chick embryos. Dev. Biol. *139*, 314–326.

Webb, D. J., Brown, C. M., and Horwitz, A. F. (2003). Illuminating adhesion complexes in migrating cells: moving toward a bright future. Curr. Opin. Cell Biol. *15*, 614–620.

Wolf, K., Mazo, I., Leung, H., Engelke, K., von Andrian, U. H., Deryugina, E. I., Strongin, A. Y., Brocker, E. B., and Friedl, P. (2003). Compensation mechanism in tumor cell migration: mesenchymal-amoeboid transition after blocking of pericellular proteolysis. J. Cell Biol. *160*, 267–277.

Yamashita, H., Goto, A., Kadowaki, T., and Kitagawa, Y. (2004). Mammalian and *Drosophila* cells adhere to the laminin alpha4 LG4 domain through syndecans, but not glypicans. Biochem. J. *382*, 933–943.